Single-Pellet, Moment Method for Analysis of Gas-Solid Reactions

A single-pellet, moment technique is presented for evaluating reaction rate constants, effective diffusivities, and adsorption equilibrium constants for gas-solid noncatalytic reactions. Experimental pulse-response data for the reaction of SO_2 with activated soda at 473 K were obtained to illustrate the method. The results show that intraparticle diffusion is the controlling mechanism for this reaction. The value of the Thiele modulus for axial transport was found to be 8.6 for a cylindrical pellet of porosity 0.56, tortuosity 2.3, and length 3×10^{-2} m.

Timur Doğu, Aliye Keskin, Gülsen Doğu
Department of Chemical Engineering
Middle East Technical University
Ankara, Turkey

J. M. Smith
Department of Chemical Engineering
University of California
Davis, CA 95616

SCOPE

Effective diffusivities of reactant and products, adsorption equilibrium and reaction rate constants are essential for the design of fluid-solid, noncatalytic reactors. The single-pellet, moment technique has been shown to be a valuable tool for evaluating effective diffusivities and adsorption parameters in porous solids (Doğu and Smith, 1975, 1976). One of the objectives of this work was to extend the application of the technique to reaction systems. The experimental procedure consists of introducing a pulse of reactive gas to one end face of a porous, cylindrical pellet of solid reactant and measuring the concentration vs. time response peak leaving the other end face. Moments of these response peaks are then equated with model equations for the moments in order to evaluate the rate and equilibrium parameters.

A gas-solid reaction that also has some potential for removal of SO_2 from flue gases is the SO_2-sodium carbonate system. When sodium bicarbonate is heated to about 473 K, a porous activated soda is produced that reacts rapidly with SO_2 (Marecek et al., 1970; T. Doğu, 1984). Pulse-response data were measured for this system to illustrate the method and to obtain values for reaction rate and diffusion parameters.

CONCLUSIONS AND SIGNIFICANCE

This work has demonstrated that gas-solid reaction rate constants together with effective diffusivities and adsorption equilibrium constants of reactant and products can be determined by the single-pellet, moment technique. Such results were obtained for the gas-solid reaction of SO_2 with activated soda at 473 K. The value of the Thiele modulus, determined from the first moment of the response curve of the product gas (CO_2), was 8.6 for a pellet of porosity 0.56 and length 3×10^{-2} m. The tortuosity factor of the pellet evaluated from inert tracer runs was 2.3. The adsorption equilibrium constant and effective diffusivity of CO_2 (in helium) were $\rho_p K_c = 0.14$ and $D_{c_{eff}} = 0.22 \times 10^{-4}$ m^2/s.

The effective diffusivity of the reactant gas (SO_2) was evaluated from the ratio of zeroth moment of the product (CO_2) response, in the reaction runs and the CO_2 response for the adsorption runs. The result, $D_{s_{eff}} = 0.23 \times 10^{-4}$ m^2/s, is larger than expected for pore-volume diffusion. Assuming that the discrepancy is due to surface diffusion of SO_2, this mechanism could contribute about 20% to the total diffusive flux in the pellet.

By carrying out the pulse-response experiments for two pellets of different lengths but with the same porosity, dead volume effects were eliminated. Analyzing the difference between the first moments for the two pellets gave more accurate values for the rate parameters than data for one pellet alone.

Introduction

Dynamic methods for the evaluation of rate and equilibrium parameters such as mass transfer coefficients, diffusivities, and adsorption rate constants are well established. The moments of the response curves to pulse inputs have been extensively used in the analysis of packed bed systems (Schneider and Smith, 1968; Hashimoto and Smith, 1973; Haynes and Sarma, 1973; Hsu and Haynes, 1981). The single-pellet, moment technique, which eliminates axial dispersion, has been used successfully for the evaluation of effective diffusivities, adsorption equilibrium, and rate constants in catalyst pellets with monodisperse and bidisperse pore structure (Doğu and Smith, 1976; Doğu and Ercan, 1983; G. Doğu, 1984).

The objective of the present research is to show that the single-pellet, moment technique also can be used for the rapid measurement of reaction rate constants, effective diffusivities of reactant and products, and adsorption parameters in gas-solid noncatalytic reactions. To demonstrate the method, experimental data were measured and analyzed for the reaction of sulfur dioxide with activated soda pellets.

Solid carbonates are frequently used for removal of SO_2 from flue gases (Hartman, 1978). Activated soda has been reported to react rapidly with sulfur dioxide, even at temperatures as low as 423 K (Marecek et al., 1970; T. Doğu, 1984). Almost complete conversion of Na_2CO_3 to the reaction products was reported. On the other hand, much lower conversion levels were obtained when limestones or dolomites were used for controlling SO_2 emission. This perhaps due to the pore-mouth closure and diffusional limitations in these reactions (Hartman and Coughlin, 1974; T. Doğu, 1981; Orbey et al., 1982).

When sodium bicarbonate is heated to a temperature of about 373 to 473 K it decomposes rapidly, forming a porous product called activated soda. The reaction is

$$2\,NaHCO_3 \rightleftharpoons Na_2CO_3 + CO_2 + H_2O \qquad [R1]$$

It is believed that the activation procedure has a significant effect on the pore structure and consequently on the activity of soda toward SO_2. The effects of temperature, gas composition, and the mechanism of the sorption reaction of SO_2 on activated soda are not well understood (Marecek et al., 1970; Genco and Rosenberg, 1976; Neuzil and Prochaska, 1978; T. Doğu, 1984).

Experimental

In this work, the dynamic version of the Wicke-Kallenbach diffusion cell was used. The details of the cell have been reported elsewhere (Doğu and Smith, 1975). Helium was used as the carrier gas flowing over the end faces of a cylindrical soda pellet. Nitrogen, carbon dioxide, and sulfur dioxide were used as the inert, adsorptive, and reactive tracers and were introduced as pulses into the stream entering the upper chamber. In the inert (N_2) and adsorbtive (CO_2) tracer runs, the response peaks measured at the outlet of the stream leaving the lower chamber were analyzed for the evaluation of the effective diffusivities and adsorption parameters. In the case of reactive (SO_2) tracer runs, sulfur dioxide reacts with activated soda and gives Na_2SO_3 (in the absence of oxygen) according to the reaction

$$Na_2CO_3 + SO_2 \rightarrow Na_2SO_3 + CO_2 \qquad [R2]$$

Part of the carbon dioxide generated by this reaction leaves the pellet from the lower face and is detected at the exit of the lower flow stream. A set of initial experiments was carried out, introducing pulses of SO_2 in the stream fed to the upper chamber, to determine the composition of the response peak. The pulse volume was 5×10^{-6} m^3. The effluent from the lower chamber was analyzed in a gas chromatograph using a Poropak Q column to separate CO_2 and SO_2. The results showed that the concentration of SO_2 leaving the lower chamber was below the limits of detection so that the response peak consisted only of the product gas (CO_2). This indicates that reaction step R2 is fast compared to diffusion in the pellet. After these initial experiments, the Poropak Q column was removed from the system and the response peaks of product (CO_2) were measured with a thermal-conductivity detector. Data were obtained for a series of lower stream flow rates. The response peaks were then analyzed for the evaluation of the rate parameters for the reaction system.

Soda pellets were prepared from sodium bicarbonate powder (Mallinckrodt AR 99.7% pure). The weighed dry powder was first moistened by contacting with saturated air in a desiccator for 2 h. Then cylindrical pellets of 3×10^{-2} and 1.3×10^{-2} m length and 1.35×10^{-2} m dia. were prepared. These pellets were dried for 24 h at 313 K, and placed into the diffusion cell. The details of the experimental system are shown in Figure 1. The diffusion cell was placed in a constant-temperature oven and the pellets activated at 473 K for 2 h while helium was flowing past the upper and lower faces of the pellet at a rate of 8×10^{-6} m^3/s. The pore-volume distribution of the sodium bicarbonate and the activated soda pellets are given in Figure 8. The total porosity and the apparent density of the activated pellet are 0.56 and 1.07×10^3 kg/m^3, respectively. After the activation step, pulse-response experiments were conducted at different lower stream flow rates at 473 K. The flow rate of the upper stream was kept constant at a high value (8×10^{-6} m^3/s at 25°C, 1 atm [101.3 kPa]) during all experiments. The pressure was maintained the same on both sides of the pellet to eliminate convective transport through the pellet. The pressure difference was observed with a manometer. After obtaining equal pressures, the manometer was disconnected prior to pulse injection to eliminate any additional contribution to the dead volume.

The experimental first-moment values evaluated from the measured response peaks contain contributions from lower and upper dead volumes. To eliminate these effects, pulse-response experiments were repeated with two pellets of identical physical properties but of different lengths (1.3 and 3.0×10^{-2} m). Then the differences between the first moments obtained with these two pellets were used in the evaluation of diffusion and reaction rate parameters. The experimental values of the zeroth and first absolute moments were determined from the observed response peaks using the equations,

$$m_n = \int_0^\infty C(t)\, t^n\, dt; \qquad n = 0, 1 \qquad (1)$$

$$\mu_1 = m_1/m_0 \qquad (2)$$

Theory

For a reactive tracer (SO_2 in this work) the mass conservation equation for one-dimensional transport through the pellet is

$$\epsilon_p \frac{\partial C_s}{\partial t} = D_{s_{\text{eff}}} \frac{\partial^2 C_s}{\partial x^2} - \rho_p N_s' \qquad (3)$$

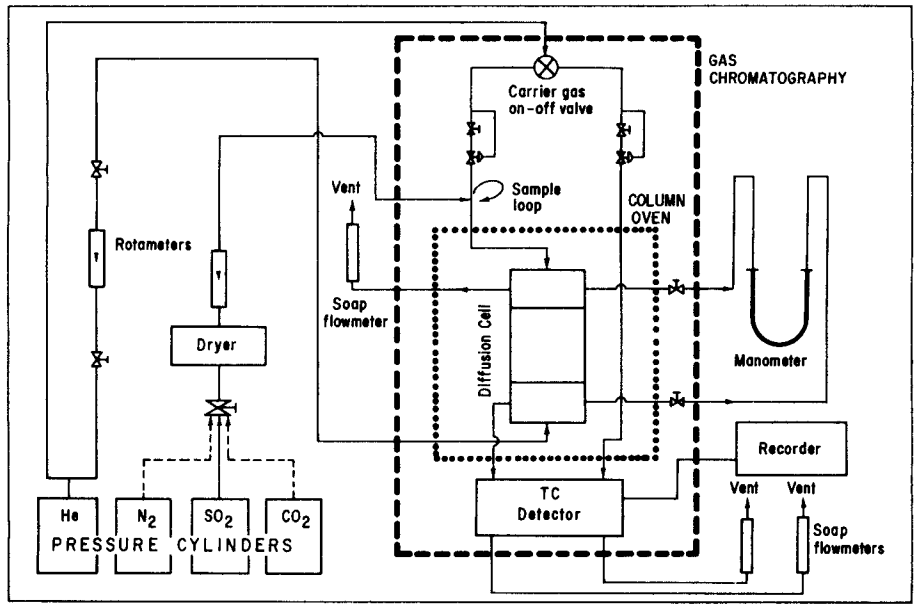

Figure 1. The experimental system.

Here, N_s' is the rate of mass transfer from the pore volume to the surface and can be expressed as

$$N_s' = kC_s + K_s \frac{\partial C_s}{\partial t} \tag{4}$$

The first term on the righthand side of Eq. 4 represents the rate of reaction (in this work the rate of R2). There are several possible mechanisms for the reaction. One is the reaction of gaseous SO_2 directly with the solid reactant without prior adsorption on the surface. Then k is the reaction rate constant of this step. A second possibility is adsorption of SO_2 followed by a surface reaction between adsorbed species and the solid. If this mechanism is correct, the rate constant k can be expressed as the product of surface reaction rate constant and the adsorption equilibrium constant, $k = k_r K$, assuming equilibrium adsorption ($n_s = KC_s$). Equation 4 and consequently the resulting moment expressions would be the same for either mechanism. The second term of Eq. 4 gives the rate of change of adsorbed-phase concentration (n_s) of reactant gas on the solid, assuming a linear equilibrium relation between the gas and adsorbed phases. Equation 4 could allow for adsorption of SO_2 on either solid phase, Na_2CO_3 or Na_2SO_3. Then K_s would be the sum of adsorption equilibrium constants on the solid reactant and solid product. In the literature, the reaction of SO_2 with activated soda has been considered to be an irreversible process under the reaction conditions; there seems to be no information available about the possible reversible adsorption of SO_2 on the solid (Marecek et al., 1970; T. Doğu, 1984).

The mass conservation equation for the product gas (CO_2) is

$$\epsilon_p \frac{\partial C_c}{\partial t} = D_{c_{\text{eff}}} \frac{\partial^2 C_c}{\partial x^2} + \rho_p N_c' \tag{5}$$

where,

$$N_c' = kC_s - K_c \frac{\partial C_c}{\partial t} \tag{6}$$

Equation 6 includes possible adsorption of the product gas (CO_2) on the solid surface.

The initial and boundary conditions for Eqs. 3 and 5 for a pulse of SO_2 introduced to the upper chamber ($x = 0$) are

$$C_s = C_c = 0 \quad \text{at} \quad t = 0 \quad \text{for} \quad 0 < x < L \tag{7}$$

Input pulse:

$$C_s = M\partial(t) \quad \text{at} \quad x = 0 \tag{8}$$

$$AD_c \left(\frac{\partial C_c}{\partial x}\right)_{x=0} = F_T C_c \quad \text{at} \quad x = 0 \tag{9}$$

$$-AD_s \left(\frac{\partial C_s}{\partial x}\right)_{x=L} = F_B C_{s_L} \quad \text{at} \quad x = L \tag{10}$$

$$-AD_c \left(\frac{\partial C_c}{\partial x}\right)_{x=L} = F_B C_{c_L} \quad \text{at} \quad x = L \tag{11}$$

In writing boundary conditions, Eqs. 10 and 11, complete mixing in the lower chamber and negligible mass transfer resistance between pellet face and gas at $x = L$ were assumed. Also the accumulation terms in the lower and upper chambers have been neglected. The restrictions are approached closely by proper design of the apparatus. The catalyst holder was designed to minimize the upper and lower volumes between the single pellet and the catalyst holder (5×10^{-7} m^3). The average residence time in the lower chamber varies from 0.25 to 0.06 s. Details of the single-pellet reactor and more information about the justification of assumptions involved in the boundary conditions were reported elsewhere (Doğu and Smith, 1975, 1976). A critical discussion of these assumptions was reported by Burghardt and Smith (1979). For high values of the top stream flow rate, the concentration of product in the top stream approaches zero ($C_c \to 0$).

First, the species conservation equation for reactant, Eq. 3

with Eq. 4, is solved in the Laplace domain with the boundary conditions stated in Eqs. 8 and 10. This solution for $\bar{C}_s$ is then substituted into the Laplace form of Eq. 6. Knowing N_c' in terms of $\bar{C}_c$, Eq. 5 can be solved in the Laplace domain for the Laplacian of the concentration of the product. Then, using the relation,

$$m_n = (-1)^n \lim_{s \to 0} \frac{d^n \bar{C}}{ds^n} \tag{12}$$

theoretical moment expressions for the product and reactant peaks are obtained. These theoretical expressions for the moments were equated to the experimental moments in order to evaluate the rate and equilibrium parameters. Since no reactant was detected at the outlet of the lower chamber, only the moment expressions for the product were used.

In the analysis of the experimental response curves for the inert (N_2) and adsorption (CO_2) pulses, the moment expressions reported in the literature (Doğu and Smith, 1976) were used. The moment expressions for all three cases, inert, adsorptive and reactive tracers, are summarized in Table 1.

Results

Effective diffusivity of N_2

Experimental values of the zeroth and first moments were computed by numerical integration of the response peaks according to Eq. 1. The pulse-response experiments conducted with the inert tracer were employed to evaluate the effective diffusion coefficient and tortuosity of the activated soda pellet. The first absolute moment values and their difference for the two pellets of identical porosity but different lengths, (pellet 1, L =

Table 1. Moment Expressions for Single-Pellet System

System	Zeroth Moment, m_0	First Absolute Moment, μ_1
Inert	$m_{0,N} = \dfrac{M \dfrac{A}{L} D_{N_{eff}}}{F_B + \dfrac{A}{L} D_{N_{eff}}}$	$\mu_{1,N} = \dfrac{L^2 \epsilon_p}{6 D_{N_{eff}}} \cdot \dfrac{\left(F_B + 3 \dfrac{A}{L} D_{N_{eff}}\right)}{\left(F_B + \dfrac{A}{L} D_{N_{eff}}\right)}$
Equilibrium adsorption	$m_{0,c} = \dfrac{M \dfrac{A}{L} D_{c_{eff}}}{F_B + \dfrac{A}{L} D_{c_{eff}}}$	$\mu_{1,c} = \dfrac{L^2}{6 D_{c_{eff}}} (\epsilon_p + \rho_p K_c) \dfrac{\left(F_B + 3 \dfrac{A}{L} D_{c_{eff}}\right)}{\left(F_B + \dfrac{A}{L} D_{c_{eff}}\right)}$
Irreversible reaction with equilibrium adsorption of reactant s and product c (for the product)	$m_{0,c} = \dfrac{M \dfrac{A}{L} D_{s_{eff}} \left[F_B (\sinh \alpha_1 - \alpha_1) \left[\dfrac{A}{L} D_{s_{eff}} \alpha_1 \cosh \alpha_1 + F_B \sinh \alpha_1 \right] + \alpha_1 \dfrac{A}{L} D_{s_{eff}} (\cosh \alpha_1 - 1) \right]}{\left[\dfrac{A}{L} D_{c_{eff}} + F_B \right]}$	$\mu_{1,c} = \dfrac{L^2}{6 D_{c_{eff}}} (\epsilon_p + \rho_p K_c) \left\{ \dfrac{6}{\alpha_1^2} \left[\dfrac{D_{c_{eff}} (\epsilon_p + \rho_p K_s)}{D_{s_{eff}} (\epsilon_p + \rho_p K_c)} - 1 \right] + \delta_1 \right\} + \dfrac{L^2}{2 D_s \alpha_1} (\epsilon_p + \rho_p K_s) \delta_2$ (General expression) $\mu_{1,c} = \dfrac{L^2}{6 D_{c_{eff}}} (\epsilon_p + \rho_p K_c) \left\{ \dfrac{6}{\alpha_1^2} \left[\dfrac{D_{c_{eff}} (\epsilon_p + \rho_p K_s)}{D_{s_{eff}} (\epsilon_p + \rho_p K_s)} - 1 \right] + \dfrac{F_B + 3 \dfrac{A}{L} D_{c_{eff}}}{F_B + \dfrac{A}{L} D_{c_{eff}}} \right\}$ (for $\alpha_1 > 7$)
Irreversible reaction with equilibrium adsorption of reactant s and product c (for the reactant)	$m_{0,s} = \dfrac{M \dfrac{A}{L} D_{s_{eff}} \alpha_1}{\dfrac{A}{L} D_{s_{eff}} \alpha_1 \cosh \alpha_1 + F_B \sinh \alpha_1}$	$\mu_{1,s} = \dfrac{L^2}{2 D_{s_{eff}} \alpha_1^2} (\epsilon_p + \rho_p K_s) \left[\dfrac{\left(\dfrac{A}{L} D_{s_{eff}} \alpha_1^2 - F_B \right) \sinh \alpha_1 + F_B \alpha_1 \cosh \alpha_1}{\dfrac{A}{L} D_{s_{eff}} \alpha_1 \cosh \alpha_1 + F_B \sinh \alpha_1} \right]$

$$\alpha_1 = L \left(\frac{\rho_p k}{D_{s_{eff}}} \right)^{1/2}$$

$$\delta_1 = \frac{F_B^2 \sinh \alpha_1 + F_B \left(\dfrac{A}{L} D_s \alpha_1 \cosh \alpha_1 - 2 \dfrac{A}{L} D_{c_{eff}} \alpha_1 + 2 \dfrac{A}{L} D_{s_{eff}} \alpha_1 + 3 \dfrac{A}{L} D_{c_{eff}} \sinh \alpha_1 \right) + 3 \left(\dfrac{A}{L} \right)^2 D_{c_{eff}} D_{s_{eff}} \alpha_1 \cosh \alpha_1}{\left(\dfrac{A}{L} D_{c_{eff}} + F_B \right) \left[F_B (\sinh \alpha_1 - \alpha_1) + \alpha_1 \dfrac{A}{L} D_{s_{eff}} (\cosh \alpha_1 - 1) \right]}$$

$$\delta_2 = \frac{\dfrac{A}{L} D_{s_{eff}} \cosh \alpha_1 + \dfrac{A}{L} D_{s_{eff}} \alpha_1 \sinh \alpha_1 + F_B \cosh \alpha_1}{D_{s_{eff}} \alpha_1 \cosh \alpha_1 + F_B \sinh \alpha_1} - \frac{\left(F_B + \dfrac{A}{L} D_{s_{eff}} \right) (\cosh \alpha_1 - 1) + \dfrac{A}{L} D_{s_{eff}} \alpha_1 \sinh \alpha_1}{F_B (\sinh \alpha_1 - \alpha_1) + \alpha_1 \dfrac{A}{L} D_{s_{eff}} (\cosh \alpha_1 - 1)}$$

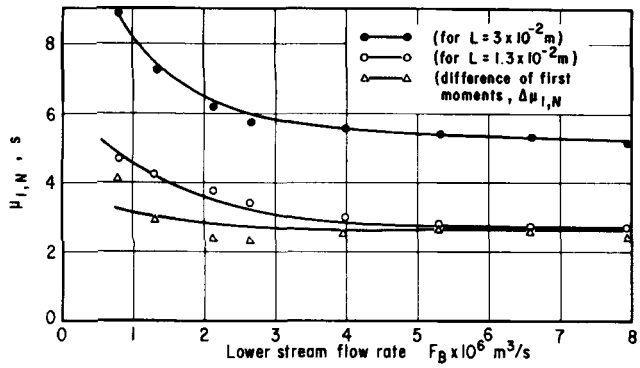

Figure 2. First absolute moment values of N_2 tracer for pellets of different lengths.

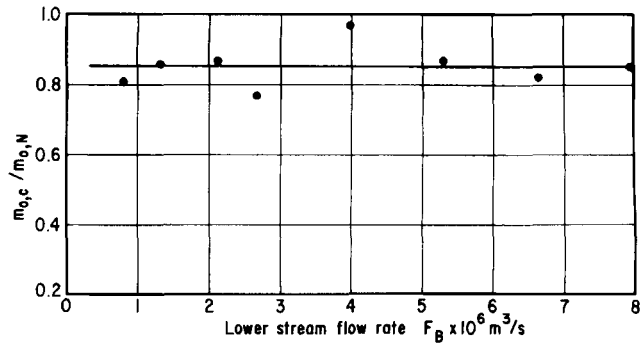

Figure 3. Ratio of zeroth moments of CO_2 and N_2 response curves.
Pellet length $L = 3 \times 10^{-2}$ m.

3×10^{-2} m; pellet 2, $L = 1.3 \times 10^{-2}$ m) are plotted in Figure 2. By taking differences the correction terms, for example, for dead volumes, cancel. Also, the flow rate dependence of the difference in first absolute moments is much less than the flow rate dependence of the first moment itself. This allows more precise evaluation of the effective diffusivity of N_2 (in helium) in the pellet. The difference of the first moments from the theoretical equations (Table 1) for an inert tracer may be expressed as

$$\Delta\mu_{1,N} = \frac{L_1^2 \epsilon_p}{6D_{N_{eff}}} \frac{\left(F_B + 3\frac{A}{L_1} D_{N_{eff}}\right)}{\left(F_B + \frac{A}{L_1} D_{N_{eff}}\right)} - \frac{L_2^2 \epsilon_p}{6D_{N_{eff}}} \frac{\left(F_B + 3\frac{A}{L_2} D_{N_{eff}}\right)}{\left(F_B + \frac{A}{L_1} D_{N_{eff}}\right)}. \quad (13)$$

For large values of the lower stream flow rate, F_B, $\Delta\mu_{1,N}$ becomes,

$$\lim_{F_B \to \infty} \Delta\mu_{1,N} = (\Delta\mu_{1,N}) = \frac{\epsilon_p}{6D_{N_{eff}}} (L_1^2 - L_2^2). \quad (14)$$

The effective diffusivity of nitrogen was calculated from the data in Figure 2 using Eq. 14. The result, which is for 473 K is 0.26×10^{-4} m^2/s.

Effective diffusivity and adsorption equilibrium constant for CO_2

The experimental values of the ratio of the zeroth moment of CO_2 to zeroth moment of N_2 are given in Figure 3. Since the sensitivity of the thermal conductivity detector is different for nitrogen and carbon dioxide, calibration runs were conducted to determine the relative magnitudes of CO_2 and N_2 peak areas for the same amount of tracer. The ratio of the experimental zeroth moment values were then corrected with this calibration factor. These corrected values, plotted as a function of lower stream flow rate in Figure 3, are essentially independent of flow rate and scatter around a mean value. The scatter of the ratio of zeroth moments is more than the first-moment results. The maximum deviation from the mean value of the ratio of zeroth moments was found to be 10%. From Table 1, the following expression represents this ratio of zeroth moments of CO_2 and N_2

$$\frac{m_{o,c}}{m_{o,N}} = \frac{D_{c_{eff}}\left(F_B + \frac{A}{L} D_{N_{eff}}\right)}{D_{N_{eff}}\left(F_B + \frac{A}{L} D_{c_{eff}}\right)} \quad (15)$$

Since the effective diffusivities of nitrogen and carbon dioxide are expected to be close, and the experimental values of lower stream flow rate were larger than the $(A/L)D_{eff}$ terms, this theoretical expression also indicates that the ratio $m_{o,c}/m_{o,N}$ should be essentially flow-rate-independent. The effective diffusivity of CO_2 is then evaluated as 0.22×10^{-4} m^2/s, as determined from the data given in Figure 3 and using Eq. 15. The experimental error involved in this value is less than 10%. This value may be checked by noting that the diffusivities should be inversely proportional to the square root of the molecular weight. Using 0.26×10^{-4} m^2/s for nitrogen, the diffusivity for CO_2 is expected to be 0.21×10^{-4} m^2/s. This agrees well with the experimental value.

First absolute moments of the response peaks obtained in experiments with CO_2 pulses are reported in Figure 4. Again, in order to eliminate the dead volume corrections, the first absolute moment values obtained with two pellets of different lengths are used in the analysis. The experimental $\Delta\mu_{1,c}$ values are some-

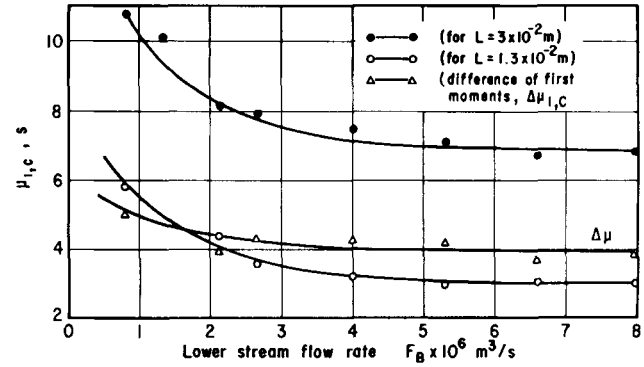

Figure 4. First absolute moment values of CO_2 tracer for pellets of different lengths.

what larger than the $\Delta\mu_{1,c}$ values predicted from Eq. 16 using the known effective diffusivity of CO_2. This result indicates that CO_2 is slightly adsorbed on the solid surface. The comparison of the CO_2 and N_2 response peaks also indicated that CO_2 peaks had a longer tail. This suggests adsorption of CO_2. Pulse-response experiments carried out at lower temperatures (about 423 K) showed that this adsorbtion phenomenon becomes more significant at lower temperatures, as expected. Considering these findings, the first-moment data of CO_2 peaks were analyzed using the equation for adsorptive tracer in Table 1. The difference of the first moments for two pellets of different lengths can then be expressed as,

$$\Delta\mu_{1,c} = \frac{L_1^2(\epsilon_p + \rho_p K_c)}{6D_{c_{\text{eff}}}} \frac{\left(3\frac{A}{L_1}D_{c_{\text{eff}}} + F_B\right)}{\left(\frac{A}{L_1}D_{c_{\text{eff}}} + F_B\right)} - \frac{L_2^2(\epsilon_p + \rho_p K_c)}{6D_{c_{\text{eff}}}} \frac{\left(3\frac{A}{L_2}D_{c_{\text{eff}}} + F_B\right)}{\left(\frac{A}{L_2}D_{c_{\text{eff}}} + F_B\right)} \quad (16)$$

For high values of F_B, $\Delta\mu_{1,c}$ becomes,

$$(\Delta\mu_{1,c\infty}) = \frac{(\epsilon_p + \rho_p K_c)}{6D_{c_{\text{eff}}}}(L_1^2 - L_2^2) \quad (17)$$

Using the data reported in Figure 4 the adsorption equilibrium constant was found as $\rho_p K_c = 0.14$.

Reaction rate and diffusion parameters for SO_2

In reaction experiments, SO_2 pulses were injected and CO_2 responses measured. The ratio of the zeroth moments of CO_2 response curves for the reaction experiments (SO_2 pulse) and the adsorption runs (CO_2 pulse) are plotted as a function of F_B in Figure 5. Using the equations given in Table 1, this ratio can be expressed as,

$$\frac{(m_{0,c})_{\text{reaction}}}{(m_{0,c})_{\text{adsorption}}} = \frac{D_{s_{\text{eff}}}}{D_{c_{\text{eff}}}}\left[1 - \frac{\alpha_1\left(F_B + \frac{A}{L}D_{s_{\text{eff}}}\right)}{F_B\sinh\alpha_1 + \frac{A}{L}D_{s_{\text{eff}}}\alpha_1\cosh\alpha_1}\right] \quad (18)$$

The dimensionless group α_1 is the Thiele modulus. Experimental results showing that there is no reactant gas leaving the lower face of the pellet suggest that surface reaction is very fast and diffusion is the controlling mechanism. For this condition Eq. 18 indicates that α_1 should be large. The experimental values of the ratio plotted in Figure 5 are essentially independent of flow rate for both long and short pellets. The value fluctuates around 1.06 for the long pellet, while slightly lower values were obtained for the short pellet. These results are consistent with the conclusion that α_1 is large. For large values of α_1 ($\alpha_1 > 6$) the second term in the parenthesis in Eq. 18 becomes negligible.

As discussed later, α_1 was evaluated for a pellet 3×10^{-2} m in length from the first-moment data of CO_2 response curves in the

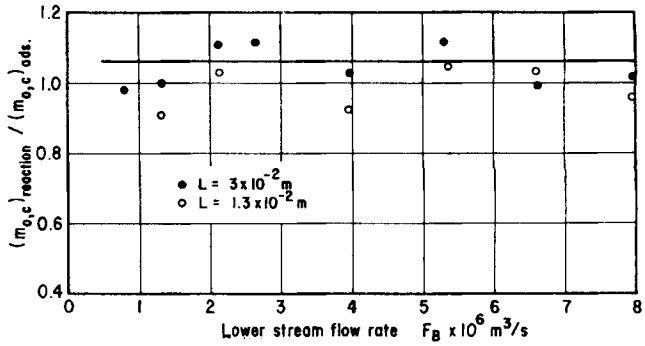

Figure 5. Ratio of zeroth moments of CO_2 in reaction (SO_2 pulse) and adsorption (CO_2 pulse) experiments.
Pellet length $L = 3 \times 10^{-2}$ m.

reaction runs. Its value was found to be 8.6. This result is consistent with the zeroth-moment data reported in Figure 5.

For α_1 values of larger than 6, Eq. 18 reduces to

$$[(m_{o,c})_{\text{reaction}}/(m_{o,c})_{\text{adsorption}}] = D_{s_{\text{eff}}}/D_{c_{\text{eff}}} \quad (19)$$

The effective diffusivity of SO_2 in helium was then calculated from the data (for the 3×10^{-2} m pellet) in Figure 5. From Eq. 19 $D_{s_{\text{eff}}} = 0.23 \times 10^{-4}$ m^2/s.

The first-moment expression for the CO_2 product in the reaction runs is given in Table 1. The difference in the first-moment expressions for the long and short pellets can be expressed as,

$$(\Delta\mu_c)_{\text{reaction}} = \frac{L_1^2}{6D_{c_{\text{eff}}}}(\epsilon_p + \rho_p K_c)\delta_{11} - \frac{L_2^2}{6D_{c_{\text{eff}}}}(\epsilon_p + \rho_p K_c)\delta_{12} + \frac{L_1^2}{2D_{s_{\text{eff}}}\alpha_{11}}(\epsilon_p + \rho_p K_c)\delta_{21} - \frac{L_2^2}{2D_{s_{\text{eff}}}\alpha_{12}}(\epsilon_p + \rho_p K_s)\delta_{22}, \quad (20)$$

where δ_{11}, δ_{21}, and α_{11} correspond to pellet 1 ($L = 3 \times 10^{-2}$ m) and δ_{12}, δ_{22}, and α_{12} correspond to pellet 2 ($L = 1.3 \times 10^{-2}$ m). The value of α_{12} is equal to α_{11} $(L_2/L_1) = 0.43\alpha_{11}$. The dimensionless groups δ_1 and δ_2 are defined in Table 1.

The first moments of the CO_2 peaks for the reaction runs for two pellets of different lengths, and the differences of the first-moment values, are given in Figure 6. The experimental first-moment values for the longer pellet were also corrected for the upper and lower dead volumes. The corrected first moments are given in Figure 7. The two unknowns, α_{11} and $\rho_p K_s$, were evaluated using the differences of first moments and the corrected first-moment values. In this analysis an iterative technique was used to evaluate the two unknowns from the two equations: Eq. 20 and the first-moment equation for the long pellet, which is

$$\mu_1 = \frac{L_1^2}{6D_{c_{\text{eff}}}}(\epsilon_p + \rho_p K_c)\delta_{11} + \frac{L_1^2}{2D_{s_{\text{eff}}}\alpha_{11}}(\epsilon_p + \rho_p K_s)\delta_{21} \quad (21)$$

The values so determined are $\alpha_{11} = 8.6$ and $\rho_p K_s = 4.2$.

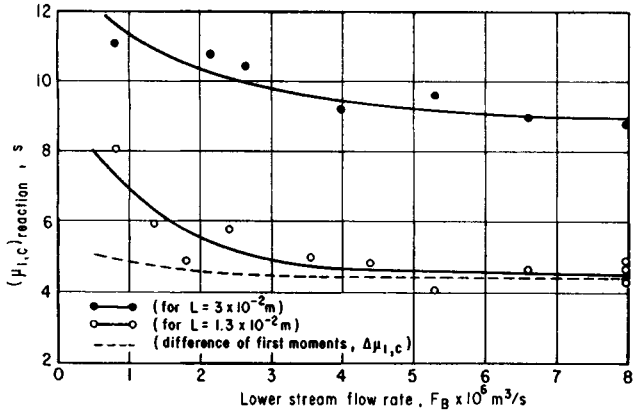

Figure 6. Experimental first absolute moment values of CO_2 in reaction experiments (SO_2 tracer injected) for pellets of different lengths.

From the definition of the Thiele modulus,

$$\alpha_1 = L\left(\frac{\rho_p k}{D_{s_{eff}}}\right)^{1/2} \tag{22}$$

and the values of α_1, L, and $D_{s_{eff}}$, $\rho_p k$ was determined to be 1.89 s^{-1}.

In the development of the theoretical moment expressions, the adsorption of SO_2 and CO_2 on the solid surface were considered to be equilibrium processes. Investigation of the derivations indicated that the first-moment expressions would not change if finite rates of reversible adsorption had been considered instead of equilibrium adsorption. Hence, the analysis presented here would still be correct. For finite reversible adsorption only the second moment expression is different from that corresponding to an equilibrium adsorption process (Doğu and Smith, 1976).

Discussion

The tortuosity of the activated soda pellet, before reaction with SO_2, can be estimated from the effective diffusivity that has been determined for N_2 (0.26×10^{-4} m^2/s). The effective diffusivity is related to a composite diffusivity, D_{i_t}, by the equation

$$D_{i_{eff}} = D_{i_t}\frac{\epsilon_p}{\tau} \tag{23}$$

where τ is the tortuosity factor. For a dilute binary system, the composite diffusivity is essentially independent of concentration and can be expressed as

$$\frac{1}{D_{i_t}} = \frac{1}{D_{i_j}} + \frac{1}{D_{i_K}} \tag{24}$$

where D_{i_j} and D_{i_K} are the molecular diffusivity of component i in j (j is the carrier gas in this work) and the Knudsen diffusivity of component i. At 473 K and 1 atm (101.3 kPa) the molecular diffusivity of N_2 in helium is estimated from the Chapman-Enskog equation to be 1.49×10^{-4} m^2/s. The Knudsen diffusivity, evaluated at the mean pore radius of 0.93×10^{-6} m, Figure 8, is 3.69×10^{-4} m^2/s. Using these values in Eqs. 23 and 24 gives a tortuosity factor of 2.3.

The ratio of the effective diffusivities of SO_2 to CO_2 was determined as 1.06 from the ratio of zeroth moments of CO_2 peaks in reaction and adsorption runs. On the other hand, the square root of the ratio of molecular weights of CO_2 and SO_2 is 0.83, suggesting some surface diffusion for SO_2. As noted earlier the effective diffusivities of N_2 and CO_2 agree with the inverse square root of the molecular weight ratio, indicating no surface transport. The effective diffusivity of SO_2 determines the amount of sulfur dioxide that enters the pellet from the top surface. Since the reaction of SO_2 with activated soda is fast, some Na_2SO_3 is expected to form near the top surface of the cylindrical pellet. Sulfur dioxide might reversibly adsorb on the Na_2SO_3 and migrate on the surface. In fact, it is reported in the literature that SO_2 reacts with Na_2SO_3 to form a stable compound, sodium pyrosulfite ($Na_2S_2O_5$) below 423 K (Kirk and Othmer, 1952; Blyakher and Laryushkina, 1962). Above this temperature $Na_2S_2O_5$ decomposes.

Additional evidence for surface transport of SO_2 is seen by comparing the predicted pore-volume diffusivity and the observed value. The effective diffusivity of SO_2 in helium predicted from Eqs. 23 and 24 is 0.18×10^{-4} m^2/s. On the other hand, the experimental value, 0.23×10^{-4} m^2/s, is larger. As shown in the previous section, the adsorption equilibrium constant of SO_2 on

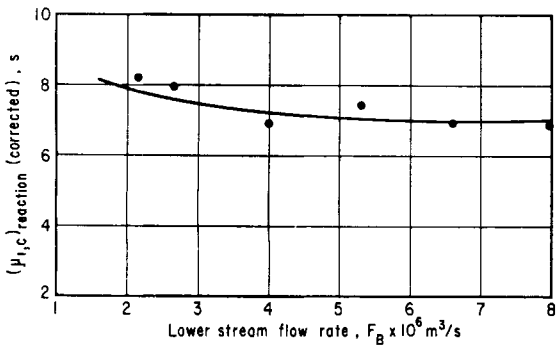

Figure 7. Corrected first absolute moment values of CO_2 in reaction experiments (SO_2 tracer injected) for pellet length $L = 3 \times 10^{-2}$ m.

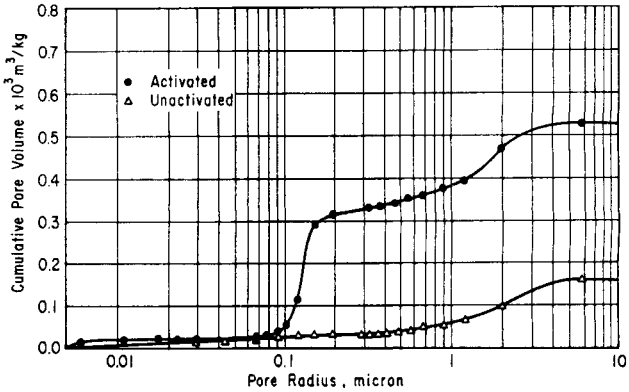

Figure 8. Cumulative pore size distribution curves for soda pellet before and after activation.

the solid surface is rather large, a necessary requirement for significant surface migration.

Figure 8 indicates that the pore structure of the pellet is bidisperse, with most of the pore volume in micropores. The effective diffusivities of N_2 and CO_2 are average values corresponding to the whole pore-size distribution. Also, in reaction runs some of the reactant solid is converted to products. Consequently the effective diffusivity of SO_2 is an average value for the whole pellet, which consists of mostly Na_2CO_3 but also contains some solid product.

The results of this work suggest that the single-pellet moment technique can be a valuable procedure for evaluating both diffusion and reaction rate parameters, as well as adsorption equilibrium constants of reactant and products, in gas-solid reactions. For large values of the Thiele modulus only the product peak was observed at the outlet of the lower stream for the SO_2-Na_2CO_3 reaction. This allowed the use of a simple thermal conductivity detector for the determination of the response peaks. For smaller values of α_1, both reactant and product peaks are expected at the outlet of the lower stream. In this case, a suitable detector such as a mass spectrometer would be required (G. Doğu, 1984) for the detection of reactant and product peaks in the presence of each other. For this situation the moment expressions for the reactant peak, given in Table 1, can be used, as well as those for the moments of the product.

Acknowledgment

This work has been supported by NATO Collaborative Research Grant No. 892/83.

Notation

A = area of end face of pellet, m^2
C_N = concentration of inert tracer (nitrogen), $kmol/m^3$
C_c = concentration of adsorbtive tracer (CO_2), $kmol/m^3$
C_s = concentration of reactive tracer (SO_2), $kmol/m^3$
C_{iL} = concentration of ith species at $x = L$, $kmol/m^3$
$D_{i_{eff}}$ = effective diffusivity of ith species, m^2/s
D_{i_t} = composite diffusivity of ith species, m^2/s
D_{iK} = Knudsen diffusivity of ith species, m^2/s
D_{ij} = molecular diffusivity of i in j, m^2/s
F_B = lower stream flow rate, m^3/s
F_T = top stream flow rate, m^3/s
k = reaction rate constant, $m^3/kg \cdot s$
K_i = equilibrium constant of species i, m^3/kg
L = length of the pellet, m
M = strength of the input pulse, $kmol \cdot s/m^3$
m_n = nth moment about the origin, Eq. 1
$m_{o,i}$ = zeroth moment of species i
s = Laplace variable, s^{-1}
x = coordinate in the direction of diffusion in pellet, m

Greek letters

α_1 = Thiele modulus defined as, $\alpha_1 = L(\rho_p^k/D_{s_{eff}})^{1/2}$
α_{1i} = value of α_1 for pellet i
$\delta(t)$ = Dirac delta pulse, s^{-1}
ϵ_p = total porosity of the pellet
μ_1 = first absolute moment, m_1/m_0, s
$\mu_{1,i}$ = first absolute moment of species, i, s
ρ_p = apparent density of the pellet, kg/m^3
τ = tortuosity factor
δ_1 = defined in Table 1
δ_{1i} = value of δ_1 for pellet i
δ_2 = defined in Table 1
δ_{2i} = value of δ_2 for pellet i

Subscripts

c = carbon dioxide
N = nitrogen
s = sulfur dioxide

Literature Cited

Blyakher, I. G., and A. G. Laryushkina, "Production of Sodium Sulfite and Pyrosulfite by Dry Process in Fluidized-Bed Reactors," *J. Appl. Chem. USSR*, **35**, 482 (1962).

Bughardt, A., and J. M. Smith, "Dynamic Response of a Single Catalyst Pellet," *Chem. Eng. Sci.*, **34**, 267 (1979).

Doğu, G. "Dynamic Single-Pellet Technique as a Tool to Analyze the Mechanism of Benzene Hydrogenation on Pt-Al_2O_3," *Proc. 8th Int. Cong. Catal.*, **3**, 155 (1984).

Doğu, G., and C. Ercan, "Dynamic Analysis of Adsorption on Bidisperse Porous Catalysts," *Can. J. Chem. Eng.*, **61**, 660 (1983).

Doğu, G., and J. M. Smith, "A Dynamic Method for Catalyst Diffusivities," *AIChE J.*, **21**, 58 (1975).

———, "Rate Parameters from Dynamic Experiments with Single Catalyst Pellets," *Chem. Eng. Sci.*, **31**, 123 (1976).

Doğu, T., "The Importance of Pore Structure and Diffusion in the Kinetics of Gas-Solid Noncatalytic Reactions: Reaction of Calcined Limestone with SO_2," *Chem. Eng. J.*, **21**, 213 (1981).

———, "Effect of Pore Structure on the Mechanism of SO_2 Sorption on Activated Soda," *Frontiers in Chemical Reaction Engineering*, R. A. Mashelkar, ed., Wiley, New York, 152 (1984).

Genco, J. M., and H. S. Rosenberg, "Sorption of SO_2 on Ground Nahcolite Ore," *J. Air Poll. Control Assoc.*, **26**, 989 (1976).

Hartman, M., "Comparison of Various Carbonates as Adsorbents of SO_2 from Combustion Gases," *Int. Chem. Eng.*, **18**, 712 (1978).

Hartman, M., and D. W. Coughlin, "Reaction of Sulfur Dioxide with Limestone and the Influence of Pore Structure," *Ind. Eng. Chem. Proc. Des. Dev.*, **13**, 248 (1974).

Hashimoto, N., and J. M. Smith, "Macropore Diffusion in Molecular Sieve Pellets by Chromatography," *Ind. Eng. Chem. Fund*, **12**, 353 (1973).

Haynes, H. W., Jr., and P. N. Sarma, "A Model for the Application of Gas Chromatography to Measurements of Diffusion in Bidispersed Structured Catalysts," *AIChE J.*, **19**, 1,043 (1973).

Hsu, L. K. P., and H. W. Haynes, Jr., "Effective Diffusivity of the Gas Chromatography Technique: Analysis and Application to Measurements of Diffusion of Various Hydrocarbons in Zeolite NaY," *AIChE J.*, **27**, 81 (1981).

Kirk, R. E., and D. F. Othmer, "Sodium Compounds," *Encyclopedia of Chemical Technology*, **12**, 612 (1952).

Marecek, J., K. Mocek, and E. Erdos, "Kinetics of the Reaction between Solid Sodium Carbonate and the Gaseous Sulphur Dioxide: Fixed Bed Reactor," *Coll. Czech. Chem. Commun.*, **35**, 1,628 (1970).

Neuzil, L., and F. Prochaska, "Fluidized Bed AKSO Process for Removing SO_2 from Gaseous Mixtures," *Fluidization*, J. F. Davidson and D. L. Keairus, eds., Cambridge Univ. Pr., 303 (1978).

Orbey, N., G. Doğu, and T. Doğu, "Breakthrough Analysis of Noncatalytic Solid Gas Reactions," *Can. J. Chem. Eng.*, **60**, 314 (1982).

Schneider, P., and J. M. Smith, "Adsorption Rate Constants from Chromatography," *AIChE J.*, **14**, 762 (1968).

Manuscript received Jan. 31, 1985, and revision received Aug. 19, 1985.